

# Synthesis and Characterization of Nanocomposites Using the Nanoscale Laser Soldering in Liquid Technique

Tran X. Phuoc<sup>\*1</sup> and Minking K. Chyu<sup>2</sup>

<sup>1</sup>Department of Energy, National Energy Technology Laboratory, University of Pittsburgh, USA

<sup>2</sup>Department of Mechanical Engineering and Materials Science, University of Pittsburgh, USA

\*Corresponding author: Tran X. Phuoc, Department of Energy, National Energy Technology Laboratory, University of Pittsburgh, P. O. Box 10940, MS 84-340, Pittsburgh, PA 15261, USA, E-mail: tran@netl.doe.gov, pxt1@pitt.edu

Citation: Tran X. Phuoc, Minking K. Chyu (2013) Synthesis and Characterization of Nanocomposites Using the Nanoscale Laser Soldering in Liquid Technique. J Mater Sci Nanotechnol 1(1): 101. doi: 10.15744/2348-9812.1.101

Received Date: June 11, 2013 Accepted Date: July 29, 2013 Published Date: August 01, 2013

## Abstract

We have synthesized Au/CuO and Au/ZnO nanocomposites using the laser soldering technique. The process was carried out by irradiating a solution containing Au-CuO and Au-ZnO nanoparticles using 532 nm laser pulses of 0.1 J/cm<sup>2</sup> continuously for 20 minutes. The beam was focused using a 75 mm focal lens and the laser power near the focal region was estimated to be about  $2.4 \times 10^{12}$  W/m<sup>2</sup>. Their UV-VIS absorption and transmission were observed and the results indicated that the bandgap energies of the Au/CuO and Au/ZnO are significantly lower than those of pure CuO and ZnO. A theoretical model was developed and the calculation showed that the soldering process was due to the laser melting of the gold nanoparticles and the molten gold got soldered to the ZnO as well as CuO nanoparticles nearby.

**Keywords:** Nanocomposite; Laser Nanosoldering

## Introduction

It is known that physical, chemical, and optical properties of semiconductors and metal nanoparticles (NPs) can be greatly enhanced if they are made in the form of alloy or core-shell nanocomposites [1-3]. Because of their composition-dependent properties, these materials can be designed to offer many advantages in environment sensing and many other industrial applications. Commonly, metal nanocomposites can be prepared using simultaneous chemical reduction of diluted metal salts in an aqueous solution composed of reducing reagents and stabilizing surfactants [4,5] or laser vaporization of metal alloys [6]. The chemical reduction method needs harmful chemicals and the produced materials are not free from being contaminated with undesired components. The laser vaporization can be used to synthesize clean nanoparticles and nanoalloys but the technique suffers from large size distributions and low yields. For these reasons, these techniques are not desirable.

In this study we report the use of the laser ablation in liquid technique to prepare Au/CuO and Au/ZnO nanocomposites. The technique is based on laser irradiation of a solution containing previously prepared nanoparticles of two types: one type of particles do not absorb the laser energy, and the other has a strong absorption band whose energy coincides with the photon energy of the laser. The particles of the former type will be unheated and remain in their solid phase. The particles of the latter type can be heated above their melting point and melted to form nanocomposites with the remaining solid particles nearby. With this approach, nanocomposites of Au/

Fe<sub>3</sub>O<sub>4</sub> [7], Au/Pt [8], Au/TiO<sub>2</sub> [9], Au/Ag [10], Au/SnO<sub>2</sub> [11], and Au/Ag, Co/Mo [12] have been successfully synthesized. In terms of the final product purity, this technique is more advantageous than the chemical one because it can generate stable nanoparticles and nanocomposites without the need of using chemical reduction reactions or ion exchange, thus, nanoparticles obtained are free of extraneous ions or other chemicals. Additional benefits can be deduced from the influence of the liquid environment which can provide further chemical effects such as oxidation, surface functionalization, etc. and physical effects such as cooling and confinement for size and size distribution control.

In the next sections, our preliminary results will be discussed. A simple theoretical model for particle temperature calculation will be also presented.

## Experiment

We first prepared, in separate vessels, Au, CuO, and ZnO nanoparticles by laser ablating gold, copper, and zinc targets, respectively, submerged in water containing 0.1 % by weight chitosan. A picture of the present experiment is shown in Figure 1. The laser beam, (0.177 J/cm<sup>2</sup> at 1064 nm, 10 Hz rep rate and 5 ns pulse duration) from a single-mode, Q-switched Nd-Yag laser was horizontally aligned 10 mm below the liquid surface and focused onto the metal target using a 50 mm focal lens.

**Two mixed solutions were prepared:** One contains Au-CuO and the other contains Au-ZnO by simply mixing the previously prepared suspensions together. The mixed solutions were then irradiated by 532 nm laser pulses of 0.1

J/cm<sup>2</sup> continuously for 20 minutes. The beam was focused using a 75 mm focal lens and the laser power near the focal region was estimated to be about  $2.4 \times 10^{12}$  W/m<sup>2</sup>. Since the gold particles had a strong Plasmon absorption band near 520 nm, they were heated, melted to form alloys with CuO, and ZnO nearby. The synthesized nanocomposites were carefully sampled for UV-VIS spectroscopy characterization using an OceanOptics CHEMUSB4000 UV/VIS/NIR spectrometer

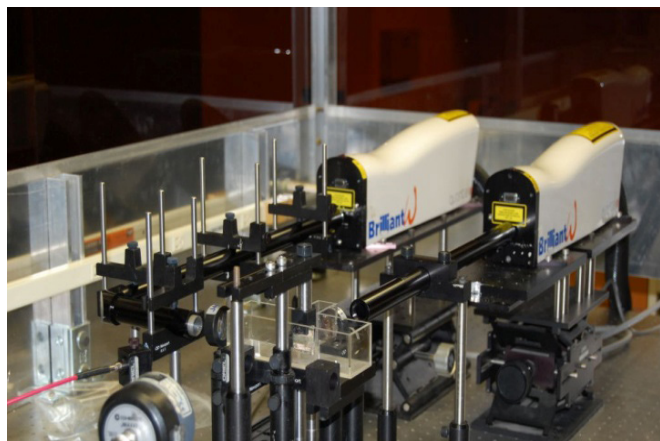


Figure 1: A picture of the laser ablation apparatus

For the alloying process mentioned above to be effective, Au nanoparticles must be in contact or in a very close proximity with CuO, and ZnO nanoparticles. The latter requires high particle density. The problem with using high particle density is that, the penetration length of the laser beam is short and many Au particles might remain unheated. To avoid such the problem, we used suspensions with low particle density and the mixed solutions were stirred at 65 RPM for 2 hours to bring the Au particles into contact with CuO and ZnO particles before being irradiated.

## Results and Discussions

Typical Au, CuO, and ZnO nanoparticles suspensions and their corresponding UV-VIS absorption spectra are shown in Figure 2. The gold nanoparticles ablated in water turned dark red while for copper and zinc, the suspensions remained colorless but they turned light-green and light-yellow, respectively after about five minutes of ablation.

The absorption spectrum of ZnO nanoparticles was significant in the wavelength region that is shorter than 450 nm and it decays quickly toward the longer range. The absorption here can be attributed to the direct/indirect transition of the ZnO electrons from the interbands residing in the deep level of the valence band. For Au and CuO suspensions, such similar transitions were observed. In addition, we also observed two intense absorption peaks: one occurred at about 520 nm for Au nanoparticles and the other around 750 nm for CuO nanoparticles. These absorption peaks can be attributed to the transition of the electrons of these materials from the upper levels of the valence band. This is also known as surface plasmon resonance peak which arises from the coherent oscillation of the Au electrons and CuO electrons by the interacting electromagnetic field.

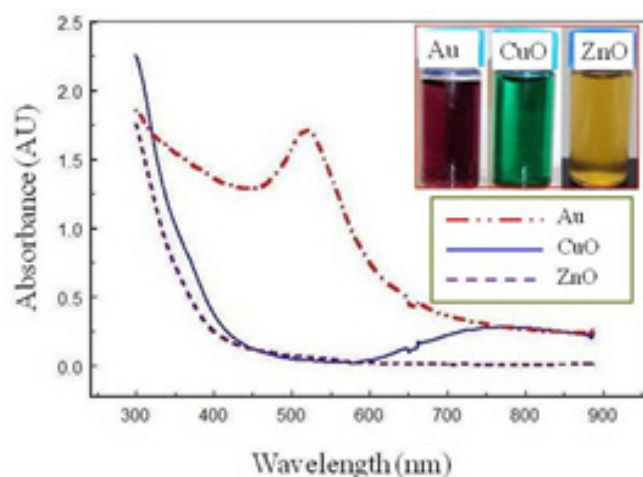


Figure 2: UV-VIS absorption Spectra of Au, CuO, and ZnO nanoparticles suspensions

The UV-VIS spectra of the mixed Au- ZnO nanoparticles suspensions and Au-CuO nanoparticles suspensions before and after being irradiated by 532 nm laser pulses are shown in Figure 3. The results shown here indicated that, before irradiation the absorption spectra of the mixed suspensions exhibited a similar behavior to that of the absorption spectra that would be obtained by summing the individual absorption spectrum shown in Figure 2. The two plasmon peaks were seen to be slightly broadened but they still located at the same locations as those shown in Figure 2. After irradiation, however, the plasmon peak due to Au nanoparticles almost disappeared indicating a significant spectral change of the suspensions after it was irradiated. Similar spectral changes were also reported by Kawaguchi et al. [7] on gold/iron oxide nanocomposites, Mafune et al. [8] on the laser nanosoldering of Au-Pt nanoparticles, and Fazio et al. [9] on the the formation of Au/TiO<sub>2</sub> nanostructures. In our case, such the spectral change must be due to the fact that, during irradiation, the gold nanoparticles were heated, melted, and different-structured nanocomposites are formed when the molten gold got soldered to the ZnO as well as CuO nanoparticles. On the other hand, if the gold nanoparticles were just simply fractured into smaller-size particles due to 532 nm irradiation, a sharper and blue-shifted plasmon peak would have been seen in the absorption spectrum.

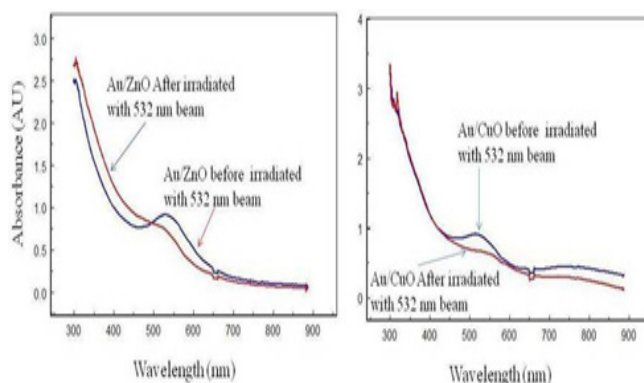


Figure 3: UV-VIS absorption spectra of Au-CuO, Au-ZnO nanoparticles suspensions before and after irradiation by 532 nm laser pulses

Another evidence of the soldering is the decrease of the bandgap energies of ZnO, CuO when they were made in the form of Au/ZnO, and Au/CuO nanocomposites. To calculate the bandgap energy, we used the Tauc equation as  $(\alpha h\nu)^n = h\nu - E_g$ . Where  $\alpha$  is the absorption coefficient,  $h$  is the Planck constant,  $\nu$  is the incident photon frequency,  $E_g$  is the bandgap energy, and  $n$  is the exponent that determines the type of the electronic transition and its values of  $1/2$  representing the indirect transition and 2 for direct transition. The absorption coefficient  $\alpha$  is determined using the Lambert-Beer-Bouguer law and it is expressed as  $\alpha = \ln(T_1/T_2)/(L_2 - L_1)$ , where  $T_1$  and  $T_2$  are the transmittances of a beam of light through a medium of length  $L_1$  and  $L_2$ , respectively. We measured the transmission spectra of ZnO, CuO, Au/ZnO, and Au/CuO composites through  $L_1 = 10$  mm and  $L_2 = 2$  mm and their corresponding absorption coefficients  $\alpha$  were determined. The results together with  $(\alpha h\nu)^2$  versus  $h\nu$  are shown in Figure 4 showing a perfect linear relationship between  $(\alpha h\nu)^2$  and the incident photon energy  $h\nu$ . This indicates that the optical bandgaps of these nanoparticles are due to a direct-allowed transition. The optical bandgap energies are determined from the intercept of the straight line with the  $h\nu$ -coordinate. The result shown here indicates that the bandgap energies for ZnO and CuO could be reduced significantly if they are made in the form of nanocomposites.

To see if the laser soldering process discussed above really happens, we developed a simple model to calculate the particle temperature when it is irradiated by a laser beam. To do so, we consider a system consisting of an isolated nanoparticle which is surrounded by water. When it interacts with a laser beam, it is heated and, as its temperature increases, thermal transport at the particle-water interface ensues. Since the pulse duration used in our experiment is 5 nanosecond which is much longer than the characteristic time of the electron-phonon scattering (about 1.7 ps [13]), the electron and phonon temperatures are uniform. In addition, since the thermal conductivity of gold and other metals is significantly high compared to that of water, temperature distribution throughout the particle volume is neglected. Thus, the laser heating of the isolated particles is described as

$$\rho_p c_{p,p} V_p \frac{dT_p}{dt} = \pi R^2 Q_{abs} I_o - Q_{l,R} \quad (1)$$

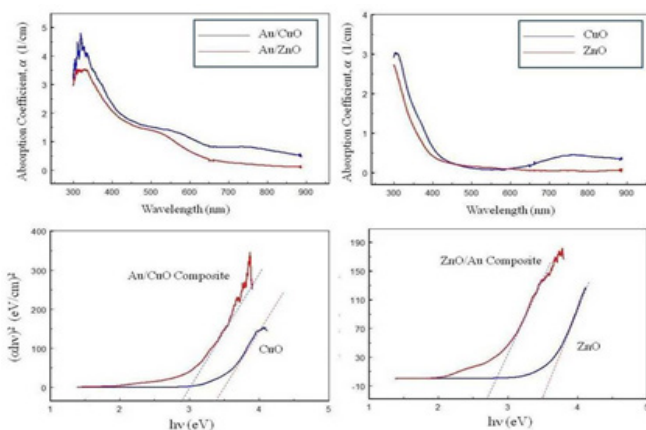


Figure 4: Bandgap energies of CuO and ZnO nanoparticles and Au/CuO and Au/ZnO nanocomposites

Where  $Q_{abs}$  is the absorption efficiency of the particle and  $Q_{l,R}$  is the heat loss from the particle surface,  $\rho_p$  is the particle density,  $c_{p,p}$  is the particle specific heat,  $V_p$  is the particle volume,  $T_p$  is the particle temperature,  $I_o$  is the laser power, and  $t$  is time. Due to the acoustic and diffusion mismatch, the particle-water interface has a thermal resistance. As a result, the thermal transport is reduced and a temperature “jump” exists across the interface. Thus, the water temperature at the particle surface,  $T_{w,R}$  must be different and less than the particle temperature  $T_p$ . The heat transport at the interface is calculated as

$$Q_{l,R} = 4\pi R^2 G(T_p - T_{w,R}) \quad (2)$$

Where  $G$  is the thermal conductance across the interface. For gold nanoparticles from 5 to 50 nm in water,  $G$  is the range from 60 to 600 MW/(m<sup>2</sup> K) were reported by Siems et al. [14]. Plech et al. [15] also reported a value of about 120 MW/(m<sup>2</sup> K) and 130 MW/(m<sup>2</sup> K) for gold and platinum nanoparticles in water, respectively.

For nanoparticles significantly less than the incident wavelength ( $2R \ll \lambda$ , or roughly  $2r < \lambda \max/10$ ) The absorption efficiency predicted by the Mie theory reduces to [16]

$$Q_{abs} = \frac{24\pi R}{\lambda} \frac{\epsilon_i \epsilon_{w,r}^{3/2}}{(\epsilon_r + 2\epsilon_{w,r})^2 + (\epsilon_i)^2} \quad (3)$$

Where  $R$  is the particle radius,  $\lambda$  is the wavelength,  $\epsilon_r$  and  $\epsilon_i$  are the real and imaginary parts of the dielectric function of the particle and  $\epsilon_{w,r}$  is the real part of the dielectric constant of water. Use of equations (2) and (3), equation (1) becomes

$$\frac{dT_p}{dt} = \frac{18\pi}{\lambda \rho_p c_{p,p}} \frac{\epsilon_r \epsilon_{w,r}^{3/2}}{(\epsilon_r + 2\epsilon_{w,r})^2 + (\epsilon_i)^2} I_o - \frac{3G}{R \rho_p c_{p,p}} (T_p - T_{w,R}) \quad (4)$$

Since the heating of the nanoparticle is fast compared to the heating of the water, a quasi-steady state can be assumed for the temperature distribution in the water and it is given as

$$\frac{d}{dr} \left( r^2 \frac{dT_w}{dr} \right) = 0 \quad (5)$$

These equations have the following initial and boundary conditions:

$$t = 0: T_p = T_w = T_o \quad (6a)$$

$$t \neq 0: \begin{cases} \left( \frac{dT_w}{dr} \right)_{r=R} = \frac{-G(T_p - T_{w,R})}{k_w} \\ T_{w,r \rightarrow \infty} = T_o \end{cases} \quad (6b)$$

Where  $k_w$  is the thermal conductivity of water. From these equations and using  $I_o$  constant throughout the heating pulse we obtained the water temperature at the interface and the time-dependent particle temperature as

$$T_{w,R} = \frac{GRT_p + k_w T_o}{k_w + GR} \quad (7)$$

$$T_p = T_o + \frac{6\pi R(k_w + GR)\epsilon_i \epsilon_w^2 I_o}{Gk_w \lambda \left[ (\epsilon_r + 2\epsilon_{w,r})^2 + (\epsilon_i)^2 \right]} \left\{ 1 - \exp\left( -\frac{3Gk_w t}{R\rho_p c_{p,p}(k_w + GR)} \right) \right\} \quad (8)$$

Using equation (8), the gold and copper particle temperatures at the end of the laser pulse were calculated and the results are tabulated in Table 1 for the laser power level used in this present experiment. Since we need to see how high the temperature could reach for a given laser power, we ignored the particle melting and let its temperature continue to rise throughout the heating pulse. The calculations were carried out for two particle sizes (R = 2.5 and 5 nm) representing the typical particle size range observed for our ablated nanoparticles and two levels of the thermal conductance at the interface, (60 and 120 MW/m<sup>2</sup> K) covering the thermal conductance range reported by Siems et al. [14] and Plech et al. [15].

G(MW/m <sup>2</sup> . K)	Tp,Au(K)		Tp,Cu(K)	
	2.5nm	5.0nm	2.5nm	5.0nm
60	1388	2300	364	447
120	977	1867	338	402

Table 1: Calculated Au and Cu particle temperatures for different particle radius and interface heat transport, (Optical properties for gold and copper from Johnson and Christy [17],  $\epsilon_{w,r}=2.63$ ,  $I_o=2.4 \times 10^{12}$ , pulse duration  $\tau=5$ ns)  $k_w=0.6$  W/m-K,  $C_{p,Au}=4689.77$  J/kg-K,  $\rho_{Au}=19300$  kg/m<sup>3</sup>,  $C_{p,Cu}=3850$  J/kg-K,  $k_w=0.6$  W/m-K,  $\rho_{Cu}=8920$  kg/m<sup>3</sup>

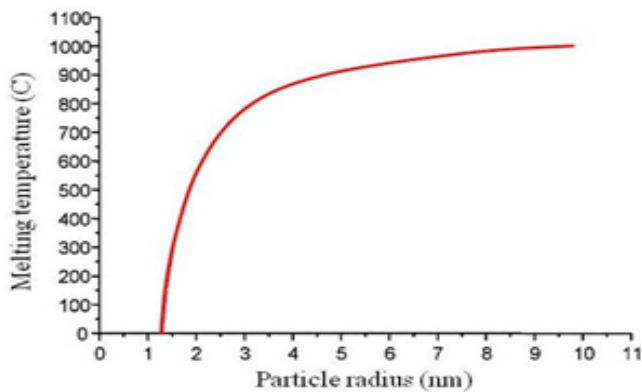


Figure 5: Melting temperature of gold nanoparticles [18]

Since, as shown in Figure 2, the absorption band of copper is in the region of about 750 nm which is very much longer than that of the laser heating beam, the laser beam had a little effect on the copper particle whose temperatures were seen to increase slightly higher than its initial value of 300 K for all conditions used here. Therefore, the copper particle remained in the solid phase throughout the heating pulse. However, for the gold nanoparticle, due to its strong absorption behavior near 520 nm, it was heated and its temperature increased significantly. For G = 60 MW/m<sup>2</sup> K, the temperatures of particle with R = 2.5 and R = 5 nm all reached higher than the melting temperature (1337 K) of the bulk gold. For G = 120 MW/m<sup>2</sup> K, the temperature was 1867 K for R = 5 nm and it was 977 K for R = 2.5 nm which is lower than the melting temperature of the bulk gold. However, it is known that melting temperature of nanoparticles decreases significantly as the size decreases. For gold, as shown in Figure 5, the melting temperature of particle

of R = 2.5 nm is about 700C (973 K) which is lower than the calculated temperature of 977 K as reported in Table 1. Thus, our simple calculation has shown that the present experiment conditions of laser power and wavelength are sufficient to heat and melt the gold nanoparticles while others are not affected and remain in their solid forms. Melting of one type of particles and keeping the others in their solid phase are required for particle soldering or alloying to ensue.

### Conclusion

We have conducted a study on the synthesis of metal nanocomposites by using the laser soldering in liquid technique. Our results on Au/CuO and Au/ZnO showed that the band-gap energies of CuO and ZnO can be tuned and significantly reduced if these metal oxides are fused with gold in the form of nanocomposites. The soldering was demonstrated using the spectral change of the synthesized nanocomposites and by a simple mathematical calculation. The process requires the melting of one particle type and keeping the other particle type in its solid form.

Our calculations indicated that larger particles are heated to higher temperature than smaller particles, therefore, it can be said that laser soldering process might be more effective if large particles are used. In addition, since the melting particle must fuse onto the solid one in order to form a nanocomposite, they have to be in contact or in a very close proximity with each other. The latter requires high particle density which, in turns, affects the laser heating process. Thus, determining the particle density for effectively soldering is necessary. Although the presence of the liquid environment could cause some additional chemical and physical effects on the synthesized nanocomposites, it is not clear at present that the laser soldering in liquid can produce nanocomposites with better physical properties than other conventional techniques. These issues are being studied and the results will be reported in our future work.

$C_{p,p}$	particle specific heat, (J/kg-K)
G	particle-water interface thermal conductance, (W/m <sup>2</sup> -K)
$I_o$	laser power, (W/m <sup>2</sup> )
$K_w$	thermal conductivity of water, (W/m-K)
$Q_{abs}$	absorption efficiency
$Q_{lr}$	heat loss from the particle surface, (W)
R	particle radius, (m)
$T_p$	particle temperature, (K)
$T_o$	initial temperature, (K)
$T_w$	water temperature, (K)
$T_{w,r}$	water temperature at the particle surface, (K)
t	time, (s)
$V_p$	particle volume, (m <sup>3</sup> )
$\epsilon_r$	real part of the dielectric function of the particle
$\epsilon_i$	imaginary part of the dielectric function of the particle
$\epsilon_{w,r}$	real part of the dielectric constant of water
$\lambda$	laser wavelength, (m)
$\lambda$	laser wavelength, (m)
$\rho_p$	particle density, (kg/m <sup>3</sup> )

## Disclaimer

"This report was prepared as an account of work sponsored by an agency of the United States Government. Neither the United States Government nor any agency thereof, nor any of their employees, makes any warranty, express or implied, or assumes any legal liability or responsibility for the accuracy, completeness, or usefulness of any information, apparatus, product, or process disclosed, or represents that its use would not infringe privately owned rights. Reference herein to any specific commercial product, process, or service by trade name, trademark, manufacturer, or otherwise does not necessarily constitute or imply its endorsement, recommendation, or favoring by the United States Government or any agency thereof. The views and opinions of authors expressed herein do not necessarily state or reflect those of the United States Government or any agency thereof".

## References

1. Yu K, Wu Z, Zhao Q, Li B, Xie Y (2008) High-temperature stable Au@SnO<sub>2</sub> core/shell supported catalyst for CO oxidation. *J Phys Chem C* 112: 2244-2247.
2. Oldfield G, Ung T, Mulvaney P (2000) Au@SnO<sub>2</sub> core-shell nanocapacitors. *Advanced Materials* 12: 1519-1522.
3. Kim Y, Johnson RC, Hupp JT (2001) Gold nanoparticle-based sensing of "spectroscopically silent" heavy metal ions. *Nano Letters* 1: 165-167.
4. Han SW, Kim Y, Kim K (1998) Dodecanethiol-Derivatized Au/Ag Bimetallic Nanoparticles: TEM, UV/VIS, XPS, and FTIR Analysis. *J Colloid Interface Science* 208: 272-278.
5. Link S, Wang ZL, El-Sayed MA (1999) Alloy formation of gold-silver nanoparticles and the dependence of the plasmon absorption on their composition. *J Phys Chem B* 103: 3529-3533.
6. Papavassiliou GC (1976) Surface-Plasmons in small Au-Ag alloy particles. *J Phys F- Met Phys* 6: L103.
7. Kawaguchi K, Jaworski J, Ishikawa Y, Sasaki T, Koshizaki N (2006) Preparation of gold/iron oxide composite nanoparticles by laser-soldering method. *IEEE Transactions on Magnetics* 42: 3620-3622.
8. Mafune F, Kohno J, Takeda Y, Kondow T (2003) Nanoscale soldering of metal nanoparticles for construction of higher-order structures. *J AM Chem Soc* 125: 1686-1687.
9. Fazio E, Calandra P, Liveri VT, Santo N, Trusso S (2011) Synthesis and physico-chemical characterization of Au/TiO<sub>2</sub> nanostructures formed by novel "cold" and "hot" nanosoldering of Au and TiO<sub>2</sub> nanoparticles dispersed in water. *Colloids and Surfaces A: Physicochemical and Engineering Aspects* 392: 171-177.
10. Chen YH, Yeh CS (2001) A new approach for the formation of alloy nanoparticles: laser synthesis of gold-silver alloy from gold-silver colloidal mixtures. *Chem Commun* 4: 371-372.
11. Bajaj G, Soni RK (2011) Gold/tin oxide nanocomposite by nanojoining. *The Open Surface Science Journal* 3: 65-69.
12. Zhang J, Worley J, Denomme S, Kingston C, Jakubek ZJ, et al. (2003) Synthesis of metal alloy nanoparticles in solution by laser irradiation of a metal powder suspension. *J Phys Chem B* 107: 6920-6923.
13. Baffou G, Rigneault H (2011) Femtosecond-pulsed optical heating of gold nanoparticles. *Phys Rev B* 84: 035415.
14. A Siems, Weber SAL, Boneberg J, Plech A (2011) Thermodynamics of nanosecond nanobubble formation at laser-excited metal nanoparticles. *New J Phys* 13: 043018.
15. Plech A, Kotaidis V, Gresillon S, Dahmen C, von Plessen G (2004) Laser-induced heating and melting of gold nanoparticles studied by time-resolved x-ray scattering. *Phys Rev B* 70: 195423.
16. Bohren CF, Huffman DR (1983) Absorption and Scattering of Light by Small Particles. John Wiley & Sons, New York, USA.
17. Johnson PB, Christy RW (1972) Optical constants of the noble metals. *Phys Rev B* 6: 4370-4379.
18. Castro T, Reifemberger R, Choi E, Andres RP (1990) Size-dependent melting temperature of individual nanometer-sized metallic clusters. *Phys Rev B* 42: 8548-8556.

Submit your next manuscript to Annex Publishers and benefit from:

- ▶ Easy online submission process
- ▶ Rapid peer review process
- ▶ Online article availability soon after acceptance for Publication
- ▶ Open access: articles available free online
- ▶ More accessibility of the articles to the readers/researchers within the field
- ▶ Better discount on subsequent article submission

Submit your manuscript at

<http://www.annexpublishers.com/paper-submission.php>